

## THE RATE OF NUCLEI FORMATION OF ZSM-5 ZEOLITE

Kyeonghwan Chung, Keunshik Kim and Gon Seo\*

Department of Chemical Technology, Chonnam National University, Kwangju 500-757, Korea

(Received 3 March 1992 • accepted 10 July 1992)

**Abstract**—The crystallization processes of ZSM-5 zeolite from mixture of colloid silica, sodium aluminate, sodium hydroxide and tetrapropyl ammonium bromide at 150-195°C were studied. As the temperature increases, crystallization time decreases, crystal size becomes smaller, and the distribution becomes narrower. The rate of nuclei formation is deduced from the size distribution of final product under the assumption that crystal is growing at constant rate from the nuclei formed during the induction period. The rate of nuclei formation is also accelerated with temperature increase. When the rate constants of the crystal growth are  $0.012\text{-}0.170 \mu\text{m}\cdot\text{min}^{-1}$  at 150-195°C, the crystallization curves can be simulated with the rate equation of nuclei formation deduced from the crystal size distribution of the final product.

### INTRODUCTION

ZSM-5 zeolite is a valuable catalyst widely used for the reactions such as conversion of methanol [1-3], alkylation of toluene [4], and isomerization of xylene [5]. Zeolite is hydrothermally crystallized from alkaline aluminosilicate solution and the crystals grow from nuclei formed at initial stage [6]. The crystallization of ZSM-5 zeolite is interesting in the aspects of high silica content and using organic template. There have been many reports [7-10] about crystallization methods and factors affecting crystal shape and composition, but only a few were related to the crystallization kinetics of ZSM-5 zeolite [11].

It is not easy to derive the rate equation of zeolite crystallization, because many factors such as temperature, composition of reactant mixture, and aging treatment, etc. are related to the rate. Furthermore, the rate of nuclei formation is required for the complete description of crystallization, while it is difficult to figure out the rate since nuclei can not be observed by conventional techniques. Therefore, the rate of nuclei formation is usually deduced from the crystal size distribution of the final product [12].

Several equations for the rate of nuclei formation are discussed [13]. Some of them are semi-theoretical equations derived from Gibbs free energy [6] or from solubility [14], while others are empirical ones based on the size distribution of final product [6].

We reported previously that it is possible to simulate the crystallization curve by using the fraction of soluble species and the induction period determined experimentally, when the linear growth rate constant of ZSM-5 zeolite is independent of crystal size [15]. In this study, we are going to discuss the nucleation rate of ZSM-5 zeolite. Applying the constant rate for linear crystal growth, the rate for the nuclei formation is deduced from the particle size distribution of crystals obtained at the end of the crystallization process. And the whole crystallization process is simulated from the rate of the nuclei formation.

### EXPERIMENTAL

The crystallizations were performed using mixtures of  $10\text{TPABr-4.5Na}_2\text{O-90SiO}_2\text{-Al}_2\text{O}_3\text{-3000H}_2\text{O}$ . Silicate solution was prepared by mixing the colloidal silica (LUDOX HS-40, Du Pont,  $\text{SiO}_2$  40 wt%) with the aqueous solution of TPABr (Aldrich, 98%). The reaction mixture was prepared by adding sodium aluminate solution into the silicate solution while being stirred vigorously. The mixture was transferred to nine small autoclaves with thin teflon beakers. The autoclaves containing 25 ml each of the mixture were placed in a temperature controlled oil bath. The autoclaves were taken out one by one from the oil bath at a certain time interval. The autoclaves were quenched with cold water and the product mixtures were transferred to 100 ml of distilled water. The samples washed and collected by using ultracentrifuge were dried over-

\*To whom correspondence should be addressed.

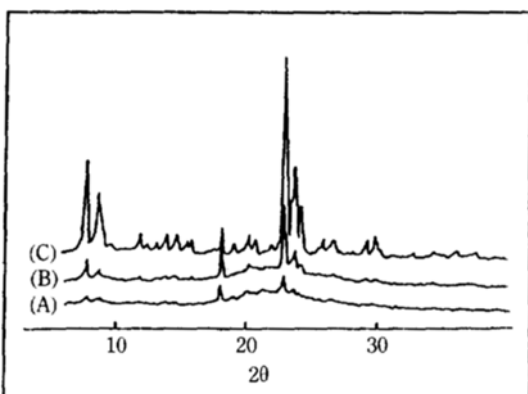


Fig. 1. Crystallization of ZSM-5 zeolite at 175°C followed by X-ray diffraction.  
(A) 120, (B) 150 and (C) 420 min.

night at 100°C.

The crystallinity and the particle size of the samples were measured by an X-ray diffractometer (Rigaku X-ray diffractometer Model Geigerflex, CuK $\alpha$ , Ni filter, 35 kV, 15 mA) and a scanning electron microscopy (JEOL JSM-35C), respectively. The particle size distribution was constructed using the results of size measurements of about 200 crystals in the final product.

## RESULTS AND DISCUSSION

Fig. 1 shows that the X-ray diffraction pattern of ZSM-5 zeolite as the crystallization proceeds at 175°C. Major peaks of ZSM-5 zeolite were observed after 120

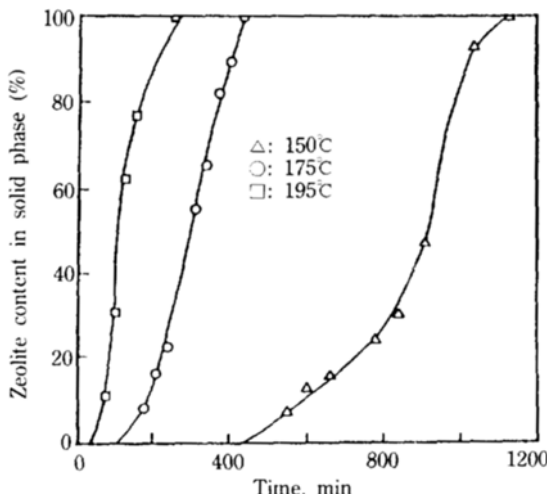


Fig. 3. Crystallization curves of ZSM-5 zeolite at various temperatures.

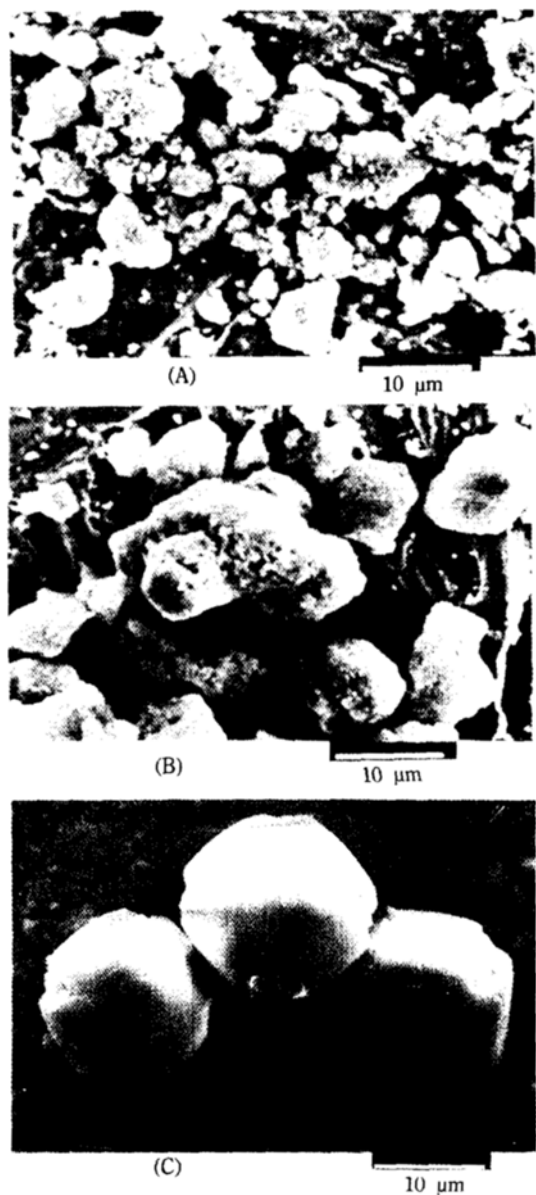


Fig. 2. Crystallization of ZSM-5 zeolite at 175°C followed by SEM photos.  
(A) 120, (B) 150 and (C) 420 min.

min, and the 20 values and relative intensities of the peaks of the sample after 420 min agreed well with those reported in literatures [10, 11]. SEM photos of the samples are shown in Fig. 2. Amorphous material gradually disappeared as the crystallization proceeded and the amount of ZSM-5 zeolite crystal increased. After 420 min, amorphous material disappeared completely.

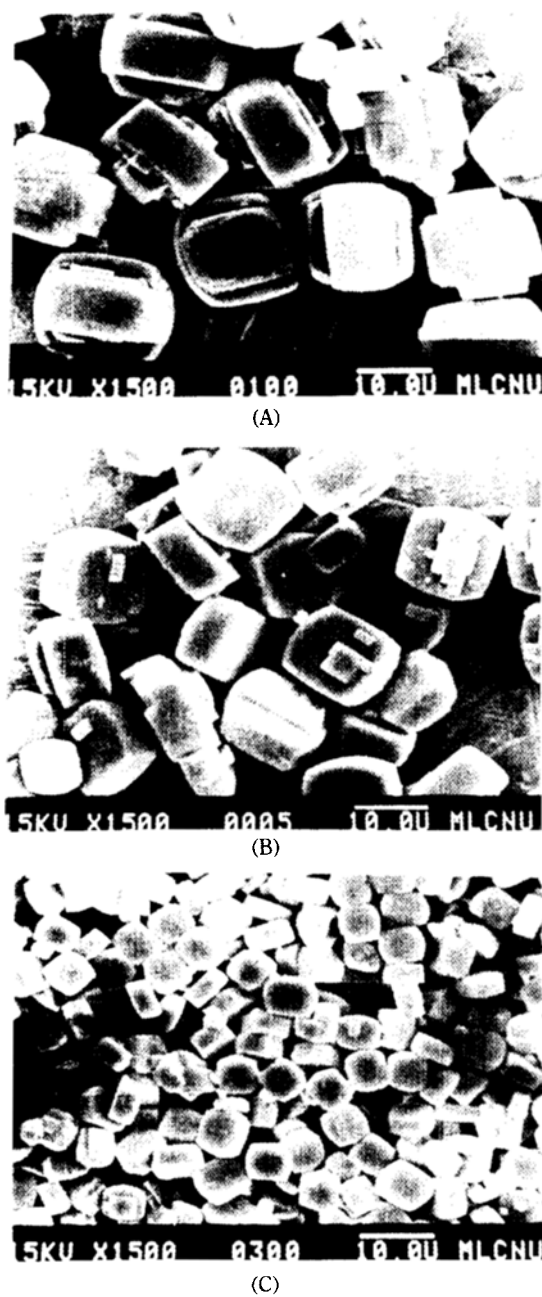


Fig. 4. Crystallization of ZSM-5 zeolite at various temperatures followed by SEM photos.

(A) 150, (B) 175 and (C) 195°C.

Crystallization curves at 150°C, 175°C and 195°C are shown in Fig. 3. The X-ray diffraction peaks of ZSM-5 zeolite were first observed after 550 min at 150°C and pure ZSM-5 zeolite was obtained after 1140 min. At elevated temperature, crystallization rate increases.

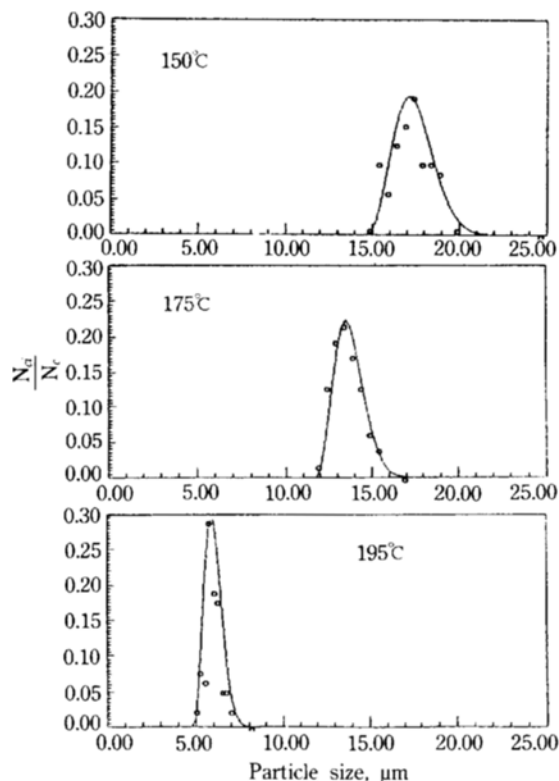


Fig. 5. Comparison of particle size distribution determined from calculated value and experimental value at various temperatures.

curve: calculated value, point: experimental value

Pure zeolite are obtained after 400 min at 175°C and after 200 min at 195°C. Since these crystallization curves match quite well with those reported [15], stirring does not seem to cause a meaningful difference on the this crystallization condition.

SEM photos of finally obtained products are shown in Fig. 4. The crystal shapes are hexagonal type as reported in literatures [16, 17]. The crystal size decreases with increase in temperature. Fig. 5 compares the crystal size distributions of the final products determined from SEM photos and calculated by the following equation of crystal size distribution;

$$\frac{n_c}{N_c} = A(l_c - l_{min})^2 \exp[-B(l_c - l_{min})^2] \quad (1)$$

where  $N_c$  is the total number of the crystals,  $n_c$  is the number of crystals with length  $l_c$ , and  $l_{min}$  is the length of the smallest crystal. This equation is modified from well-known nucleation rate equation of zeolite,  $dN/dt = At^b \exp(-t^n)$  [6]. Curves are determined

from Eq. (1) and points indicate experimental value in Fig. 5. The simulated curves determined from this equation agree well with experimental results. In this crystal size distribution, A and B are parameters related to amplitude and width of distribution, respectively. Selected values of A and B for best fits are listed below;

Temperature, °C	A	B
150	0.095	0.180
175	0.200	0.330
195	0.800	0.980

As the temperature increases, the values of A and B increase indicating that the width of distribution curve becomes narrower.

Nuclei are formed at the initial stage of the crystallization. If the formed nuclei grow to a certain size, they grow to crystals. However, some of them dissolve back to the solution before they grow to the certain size. In this paper, we call nuclei as those which do not dissolve and grow to final product. Assuming the nuclei are growing to final product at a constant rate, the rate of nuclei formation can be deduced from the size distribution obtained at the final time  $t_f$  [12]. The nuclei formed at  $t=t_{ni}$  (the initial time of nuclei formation) grow to crystals of  $l_{max}$  at  $t_f$ . The nuclei formed at  $t=t_{nf}$  (the final time of nuclei formation) grow to the crystals of  $l_{min}$  at  $t_f$ . Therefore, the length  $l_i$  of the crystal grown from the nuclei formed at  $t_{ni}$  ( $l_{min} < l_i < l_{max}$ ) can be expressed as a function of the time of nuclei formation  $t_{ni}$  as follows;

$$l_i(t) = k_{crys} \cdot s(t - t_{ni}) \\ = k_{app} \cdot (t - t_{ni}) \quad (2)$$

where  $k_{crys}$  is the rate constant for linear growth and  $k_{app}$  is the apparent rate constant defined as  $k_{crys} \cdot s$ . In this equation,  $s$  represents the fraction of soluble species to the sum of amorphous material, soluble species and zeolite crystal and can be deduced from crystallization curve [15]. The fraction  $s$  is constant as long as the amorphous material is remaining in the mixture, since there is an equilibrium between the amorphous material and the soluble species [18].

By substituting  $l_i$  into the Eq. (1), the fraction of nuclei as a function of the crystallization time can be expressed as follows;

$$\frac{n_{ni}}{N_n} = A \cdot k_{app}^2 (t_{nf} - t_{ni})^2 \exp[-B \cdot k_{app}^2 (t_{nf} - t_{ni})^2] \quad (3)$$

where  $N_n$  is the total number of nuclei formed and grown to final crystal and  $n_{ni}$  is the number of nuclei

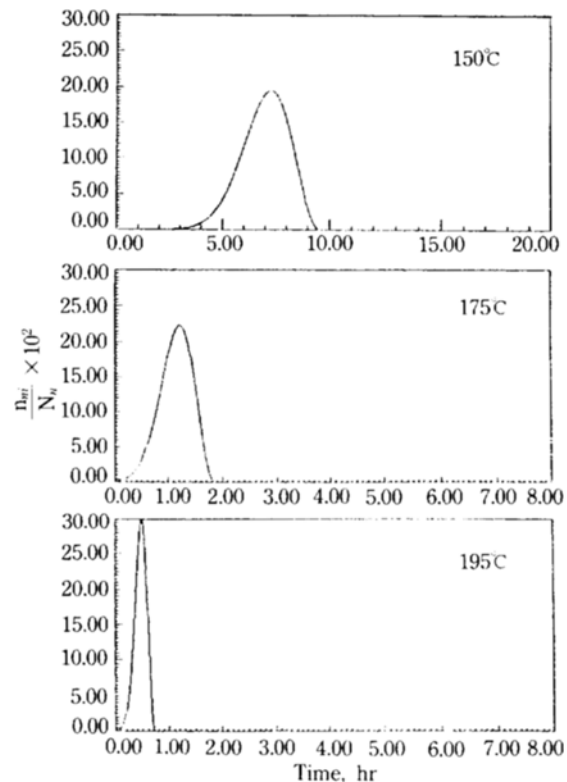


Fig. 6. Rate of nuclei formation deduced from size distribution of final product.

formed at  $t_{ni}$ ,  $t_{nf}$  can be determined from the largest crystal of final product. Therefore, the fraction of nuclei formed at  $t_{ni}$  can be calculated. Fig. 6 shows the rate of nuclei formation at various temperatures. The shapes of the curves are similar to those reported in the reference [6]. These curves show that the rate of nuclei formation becomes faster at elevated temperature and the period for nuclei formation is shortened due to fast growth of crystal, as reported by Meise and Schwochow [19] for the crystallization of zeolite A.

As zeolite is growing with a constant linear rate, the fraction of zeolite formation at  $t$  can be calculated by summation of all crystals with  $l_i(t)$  expressed by Eq. (2),

$$\frac{Z_t}{Z_f} = \frac{\sum (n_{ni}/N_n) [l_i(t)]^3}{\sum (n_{ni}/N_n) [l_i(t_f)]^3} \quad (4)$$

where  $Z_t$  and  $Z_f$  are the amounts of zeolite produced from the reaction mixture at time  $t$  and  $t_f$ , respectively.

The rate of crystal growth starts decreasing with crystallization time after the dissolution of the amorphous solid material finishes, because the concentra-

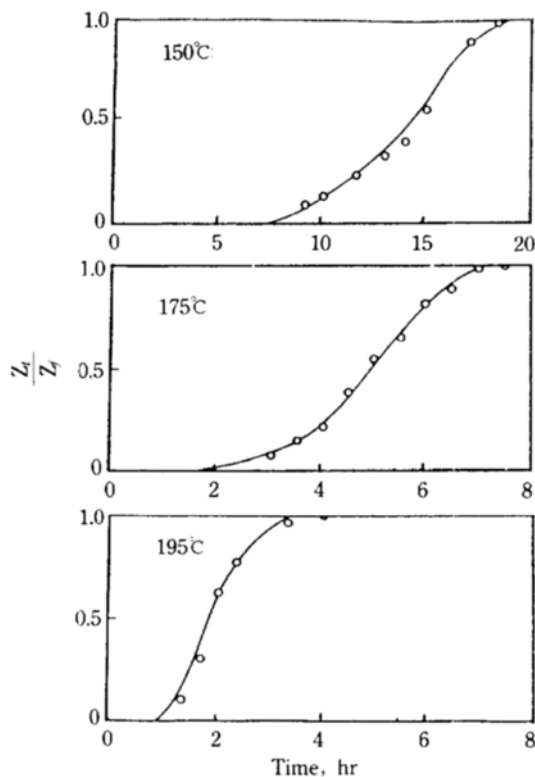


Fig. 7. Comparison of crystallization curves determined from calculated curves and experimental values at various temperatures.

curve: calculated value, point: experimental value

tion of soluble species decreases due to consumption for the growth of zeolite crystal. Therefore, the apparent rate constant of crystal growth also starts decreasing with decrease in the fraction of soluble species as shown in Eq. (5).

$$k_{app} = k_{cryst}(s - \Delta Z) \quad (5)$$

Where  $\Delta Z$  is the fraction of crystal growth indicating the consumption of the soluble species during a given time interval. As long as the amorphous solid phase remains,  $\Delta Z$  is set as zero. However, after the time  $t_a$  when all the amorphous solid phase is consumed, the decrease in the concentration of soluble species should be considered. The time  $t_a$  and the fraction of soluble species can be approximately estimated from the slope of crystallization curve, since the rate of crystal growth is decreased after the complete dissolution of all the amorphous solid phase [15].

Using Eq. (2) for  $0 < t < t_a$  and Eq. (5) for  $t > t_a$ , the crystallization curve can be calculated with  $k_{app}$  esti-

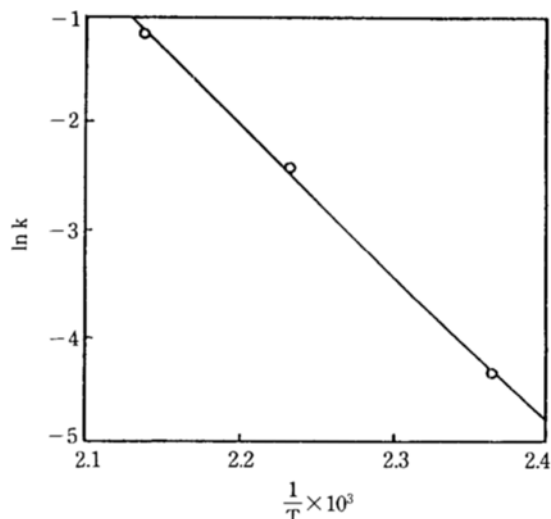


Fig. 8. Temperature dependence of rate constants for ZSM-5 zeolite crystallization determined from simulated curves.

mated from  $l_{max}/t_f$ . The value of  $k_{app}$  can be adjusted from the comparison of the simulated curve with experimental results. Fig. 7 shows the simulated curves. The simulated curves describe the experimental results fairly well. From the best fits,  $k_{cryst}$  are determined as  $0.011, 0.047, 0.120 \mu\text{m} \cdot \text{min}^{-1}$  at  $150, 175$  and  $195^\circ\text{C}$ , respectively. These values are almost the same as those obtained at stirring condition [15].

The Arrhenius plot of the rate constant of crystal growth is shown in Fig. 8. Good linearity is observed and the apparent activation energy for crystal growth is  $88 \text{ kJ} \cdot \text{mol}^{-1}$ . This value is similar to the one reported in the literature [14].

As the temperature increases, crystallization rate increases and size distribution becomes narrower. At the elevated temperature, the rate of nuclei formation becomes faster the number of the nuclei formed during the induction period increases. Since the number of nuclei is higher and crystal growth rate is faster, the crystals become smaller than those obtained at lower temperature and size distribution becomes narrower.

## CONCLUSIONS

The simulated curves of ZSM-5 zeolite agree well with experimental results. This simulation is based on the rate of nuclei formation deduced from size distribution of final product and the solution transfer mechanism with constant rate of crystal growth. The rate

of nuclei formation of ZSM-5 zeolite is accelerated with increase in temperature. Faster crystallization and narrower size distribution at elevated temperature can be explained by the increase in the rates of nuclei formation and crystal growth. While the kinetic of nuclei formation is unknown, the rate of nuclei formation deduced from the size distribution of final product is helpful in simulating the crystallization curve and determining the rate constant.

### ACKNOWLEDGEMENT

The Ministry of Education is acknowledged for support of this work.

### NOMENCLATURE

A	: constant of Eq. (1) in particle size distribution
B	: constant of Eq. (1) in particle size distribution
$k_{app}$	: apparent rate constant for zeolite growing defined as $k_{crys} \cdot s$
$k_{crys}$	: rate constant of zeolite growth
$l_c$	: the length of crystals
$l_c(t)$	: the crystal length at time t
$t_c(t_f)$	: the crystal length at time $t_f$
$l_{max}$	: length of the largest crystal of the final product
$l_{min}$	: length of the smailest crystal of the final product
$N_c$	: total number of crystals
$n_{ci}$	: number of crystals with length $l_c$
$N_n$	: total number of nuclei
$n_{ni}$	: number of nuclei formed at time $t_{ni}$
s	: fraction of soluble species in reactant
t	: crystallization time
$t_a$	: the time that all the amorphous solid phase is disappeared
$t_f$	: the final time of the crystallization process
$t_m$	: the time of nuclei formation for crystal with length $l_c$

$t_{no}$	: the initial time of nucleation
$t_{nf}$	: the final time of nucleation
Z	: fraction of zeolite
$Z_f$	: the amount of zeolite formed at end time
$Z_t$	: the amount of zeolite formed at time t

### REFERENCES

1. Chang, C. D. and Silvestri, A. J.: *J. Catal.*, **56**, 169 (1979).
2. Kaeding, W. W. and Butter, S. A.: *J. Catal.*, **61**, 155 (1980).
3. Meisel, S. L., McCullough, J. P., Lechhaler, C. H. and Weisz, P. B.: *CHEMTECH*, Feb., p.86 (1976).
4. Kaeding, W. W., Chu, C. C., Young, S. B., Weistern, B. and Butter, S. A.: *J. Catal.*, **67**, 159 (1981).
5. Morrison, R. A.: US Patent 3,856,872 (1974).
6. Barrer, R. M.: "Hydrothermal Chemistry of Zeolite", Academic Press, London, chapter 4, (1982).
7. Nastro, A. and Sand, L. B.: *Zeolites*, **3**, 57 (1983).
8. Ghamami, M. and Sand, L. B.: *Zeolites*, **3**, 155 (1983).
9. Araya, A. and Lowe, B. M.: *Zeolites*, **6**, 111 (1986).
10. Thompson, R. W. and Huber, M. J.: *J. Crystal Growth*, **56**, 711 (1982).
11. Thompson, R. W. and Dyor, A.: *Zeolites*, **5**, 292 (1985).
12. Zhdanov, S. P. and Samuelich, N. N.: Proc. 5th Intern. Conf. Zeolites, Heydn, London, p.75 (1980).
13. Thompson, R. W. and Dyor, A.: *Zeolites*, **5**, 302 (1985).
14. Chao, K. J., Tsai, T. C. and Chen, M. S.: *J. Chem. Soc., Faraday Trans.*, **1**, 77, 547 (1981).
15. Seo, G., Chung, K. H. and Park, T. J.: *Hwahak Go-nghak*, **30**, 285 (1992).
16. Argaur, R. J. and Landolt, G. R.: US Patent 3,702, 886 (1972).
17. Erdem, A. and Sand, L. B.: *J. Catal.*, **47**, 249 (1977).
18. Zhdanov, S. P.: *Adv. Chem. Ser.*, **101**, 20 (1970).
19. Meise, W. and Schwochow, F. E.: *Adv. Chem. Ser.*, **121**, 169 (1972).